

Synthesis and characterization of novel fluorescent amphiphilic diblock copolymer

B. Rajkumar¹ · T. Dhanalakshmi² · B. Meenarathi¹ ·
R. Anbarasan¹

Received: 18 January 2015 / Revised: 25 December 2015 / Accepted: 4 January 2016 /
Published online: 11 January 2016
© Springer-Verlag Berlin Heidelberg 2016

Abstract In the present study, an amphiphilic diblock copolymer made of poly(ϵ -caprolactone) (PCL) and poly(tetrahydrofuran) (PTHF) was synthesized via ring opening polymerization (ROP) of ϵ -caprolactone (CL) and tetrahydrofuran (THF) with rose bengal (RB) as a bridging agent in a two-step process. In the first step, RB–PCL was synthesized by the ROP of CL, while in the second step the diblock copolymer was prepared by the ROP of THF with RB–PCL moiety as a chemical initiator in the presence of phthalic anhydride (PAH) as a co-monomer. The diblock copolymer was characterized by ¹H and ¹³C nuclear magnetic resonance (NMR) spectroscopy, Fourier transform infra red (FTIR) spectroscopy, UV–visible spectroscopy, fluorescence spectroscopy, differential scanning calorimetry (DSC), thermogravimetric analysis (TGA), scanning electron microscopy (SEM), field emission scanning electron microscopy (FESEM), gel permeation chromatography (GPC) and EDX studies.

Keywords Amphiphilic diblock copolymer · Poly(ϵ -caprolactone) · Poly(tetrahydrofuran) · Synthesis · Characterization · Polymer nanoparticles

Introduction

Dyes are used in MRI applications as a fluorescent probe. Unfortunately, after the scanning process, such a fluorescent probe is not removed from the cells or it is not induced for its degradation by the external stimulating agents. Sometimes, the dye

✉ R. Anbarasan
anbu_may3@yahoo.co.in

¹ Department of Polymer Technology, Kamaraj College of Engineering and Technology, Virudhunagar 626 001, Tamilnadu, India

² Department of Chemistry, Kamaraj College of Engineering and Technology, Virudhunagar 626 001, Tamilnadu, India

itself is a carcinogenic one and the heavy dose leads to unwanted diseases. Moreover, the conjugation of dye molecules with a carrier material includes the consumption of a lot of hazardous solvents, loss of economy, time and consumables and is sometimes not an eco-friendly approach. This is one of the problems polymer scientists recently face. Conventional chemotherapeutic agents have certain limitations such as poor solubility of drug in an aqueous medium and their side effects. As a result, we need to search for an alternate or a new material. The above-mentioned two problems can be overcome by a simple eco-friendly method. This is the novelty of the present investigation. The present methodology follows an eco-friendly and economically cheaper approach and the dye molecule can be induced for its degradation by the carrier material itself after its utilization. Generally, the drugs are incorporated into the nanosized polymeric micelles and act as promising nanocarrier systems for drug and gene delivery. Such diblock or triblock copolymer based amphiphiles include nanosized polymeric micelles, which are a medical miracle in the drug delivery system. The induced bio-degradation of dye and nano micelles as an effective drug carrier is the key ideas of the present investigation. We have prepared such a material.

Polymeric micelles consisting of hydrophilic and hydrophobic segments have received special attention due to their potential application and academic interest in many interdisciplinary fields. The most widely studied amphiphilic polymers for drug delivery systems are diblock and triblock copolymers, because of their biocompatibility and biodegradability as well as minimum cytotoxicity. PCL is a semi-crystalline linear aliphatic polyester and has been studied intensively due to its good biodegradability, nontoxicity and biocompatibility. PCL can be prepared by the ROP of lactone. In 2013, Wang et al. [1] reported about the novel amphiphilic block copolymers for drug delivery applications. PCL and PEG based star amphiphilic block copolymers for drug carrier application were synthesized [2]. Li and co-workers [3] reported the synthesis of super paramagnetic amphiphilic copolymers. A novel polyisocyanate amphiphilic copolymer with hydroxyl side group was reported by Chen et al. [4]. Similarly, various amphiphilic copolymers have been reported in the literature [5–10]. A thorough literature survey indicates that PCL based amphiphilic copolymer reports are rarely available in the literature. This urged us toward the present investigation. The advantage of using PCL is the availability of micro pores on its surface that is used as temporary accommodation for the drug moieties.

PTHF has been synthesized via cationic ROP of THF [11]. PTHF plays a vital role in biomedical engineering as a drug carrier. Moreover, PTHF is a water soluble and biocompatible polyether. This motivated the synthesis of PTHF-based amphiphiles. Synthesis, characterization and controlled architecture of PTHF-based multiblock copolymer have been reported by Gardella et al. [12]. In 2001, Kusan et al. [13] synthesized a block copolymer comprising PTHF and one or two [5] polyurethane blocks. Diblock copolymers of poly(3-hexyl thiophene) and PTHF were synthesized via Grignard metathesis and cationic polymerization [14]. Synthesis and crystallization behavior of PTHF-based diblock copolymer were studied by Fan et al. [15]. After a thorough literature survey, we could not find any report based on the fluorescent PTHF-based amphiphilic diblock copolymers. In the

present investigation, we took this as a challenge and successfully synthesized the same.

Photodynamic therapy (PDT) is an emerging treatment used for the apoptosis of cancerous cells. For this purpose, dyes are used to generate reactive oxygen species (ROS). Among the dyes used, RB plays a vital role in PDT as a photo sensitizer [16]. RB finds application in the biochemistry field also as a staining agent [17]. RB is used to test liver disease in infancy and childhood [18]. Apart from biomedical applications, the xanthene-type dye is also useful in ROP as a catalyst [19]. In the photo-oxidation process, RB acts as a catalyst [20]. To the best of our knowledge, RB-initiated ROP of CL and THF toward the amphiphilic polymer system is not available in the literature. To achieve the target, RB is used as an initiator for the ROP of CL and THF. This methodology offers a self-alignment system leading to nanoparticle formation, which is the novelty of the present investigation. On thorough literature survey, we could not find any report based on the synthesis and characterization of amphiphilic diblock copolymer using the dye as a bridging agent.

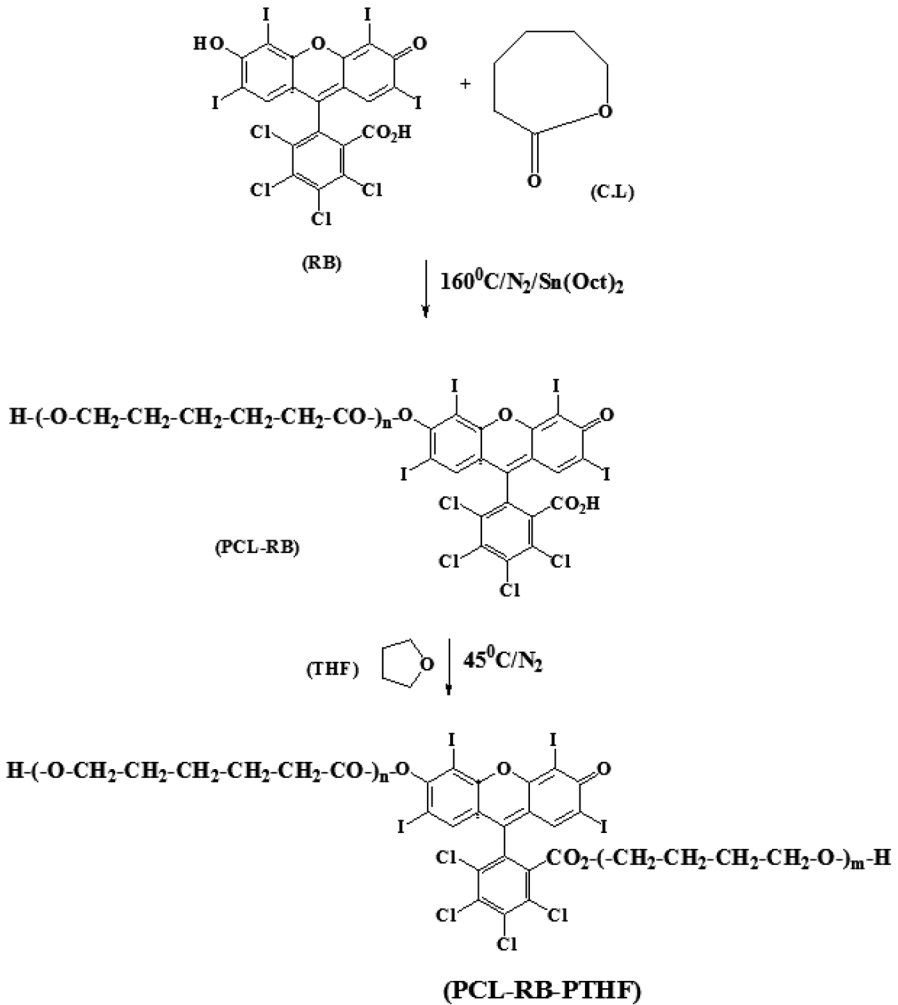
Materials and methods

Materials

ϵ -Caprolactone (CL, monomer) and stannous 2-ethyl hexanoate [$\text{Sn}(\text{Oct})_2$, catalyst] were purchased from Sigma Aldrich, India, and were used as received. Tetrahydrofuran (THF) was purchased from Merck, India, and was used as such. Rose bengal (RB, initiator), chloroform, diethyl ether and phthalic anhydride (PAH, co-monomer) were purchased from Spectrum Chemicals, India, AR grade, and were used without further purification. Double distilled water (DDW) was used for making solutions.

Step I: synthesis of the RB–PCL system

The ROP of CL with RB was carried out in the presence of $\text{Sn}(\text{Oct})_2$ as catalyst according to the literature (Scheme 1) [13]. The procedure in brief is given below: PCL was prepared by the bulk polymerization method. 4.0 g of CL was introduced into a three-necked flask containing 0.40 g of RB and 0.004 g of $\text{Sn}(\text{Oct})_2$. Here, the monomer to initiator ratio (M/I) is equal to 100, whereas the monomer to catalyst ratio (M/C) is equal to 1000. The [M/I] and [M/C] play a vital role in the molecular weight of the polymer. From the literature, it was found that while increasing the [M/I] or [M/C], the molecular weight of the polymer was increased due to the availability of lesser number of initiating species or centers. The resulting mixture was then placed in an oil bath at 160 °C and stirred slowly for 2 h under a nitrogen atmosphere. At the end of the polymerization reaction, the resulting product was cooled and dissolved in 25 mL chloroform solvent and re-precipitated by the addition of 200 mL of diethyl ether.



Scheme 1 Synthesis of PCL–RB–PTHF

Step II: synthesis of PCL–RB–PTHF diblock copolymer

About 2.0 g of the monoblock polymer of RB–PCL obtained in the previous step was dissolved in 25 mL THF. 5 mL DDW and 0.02 g of PAH were added. The mixture was then refluxed at 45 °C for about 24 h. After the reaction was over, the polymer was cooled to room temperature and evaporated to dryness. The pale brown diblock copolymer thus obtained is PCL–RB–PTHF. The polymer was dried and weighed and stored in a zipper lock bag. The reaction is mentioned in Scheme 1 [11].

Characterization

The FTIR spectra were recorded on a Shimadzu 8400 S spectrometer in the range of 400 to 4000 cm^{-1} at room temperature. The block copolymer was powdered, ground with spectral grade KBr and pelletized. The spectra were taken for samples obtained in both the synthesis steps. UV–visible spectral analysis was carried out for samples from both the synthesis steps by making a solution with THF solvent ($[\text{PCL-RB}] = 1.8 \times 10^{-6} \text{ M}$, $[\text{PCL-RB-PTHF}] = 2.2 \times 10^{-6} \text{ M}$) and then using a Shimadzu 3600 NIR Japan instrument and measurements were carried out in the range 250–650 nm. Thermal analysis of the samples was carried out using Universal V4.4A TA Instruments under a nitrogen atmosphere in a platinum pan at the heating rate of 10 $^{\circ}\text{C min}^{-1}$ from room temperature to around 800 $^{\circ}\text{C}$. Fluorescence measurements were carried out with an Elico SL 172, (India) for both samples obtained in steps I and II in THF solvent with the above-mentioned concentrations. The excitation wavelength was 310 nm. The morphology of the samples was examined using a Jeol (JMS-840) SEM instrument. The samples were coated with carbon to avoid charging under the electron beam. ^1H and ^{13}C -NMR (500 MHz) spectra were obtained using an NMR apparatus (Varian, Unity Inova-500 NMR) at room temperature in CDCl_3 solvent with tetramethylsilane as an internal reference standard. The surface morphology and particle size of the PCL-RB-PTHF polymeric nanoparticle (step II sample) were determined by FESEM, Hitachi S4800 Japan instrument. The molecular weight determinations of diblock copolymer samples were carried out in GPC, Perkin Elmer Series 200 at 30 $^{\circ}\text{C}$. THF was used as an eluent.

Results and discussion

The main aim of the present investigation is synthesis and characterization of an amphiphilic fluorescent diblock copolymer using RB as an initiator as well as bridging agent. The ROP of CL was carried out by the bulk polymerization method and is shown in Scheme 1 [11]. In the first step, the ROP of CL was carried out using RB as a lone chemical initiator. In the second step, the polymer prepared in the first step was used as an initiator for the ROP of THF and PAH as a comonomer. The polymer prepared in each step was characterized by various analytical tools to confirm the functionalities present, chemical structure, melt transition temperature (T_m) and surface morphology etc. Here, a polymer with low processing temperature was prepared and is suitable for biomedical application.

FTIR spectral study

The FTIR spectrum of RB-initiated ROP of CL and THF is shown in Fig. 1. Figure 1a indicates the FTIR spectrum of RB-conjugated PCL. The important peaks are characterized below. A broad peak around 3436 cm^{-1} explains the –OH stretching of PCL. The C–H symmetric and anti-symmetric stretching are noted at 2862 and 2943 cm^{-1} respectively. The C=O stretching appeared at 1724 cm^{-1} .

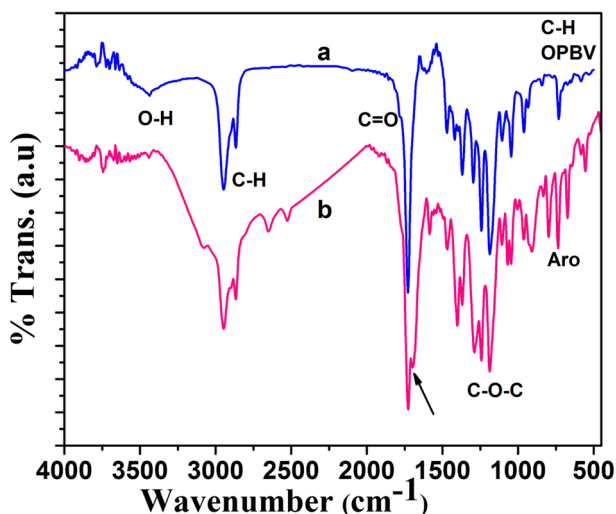


Fig. 1 FTIR spectra of RB–PCL (a) and PCL–RB–PTHF (b) systems

When Meenarathi et al. [21] synthesized PCL, they also observed the C=O stretching around 1724 cm^{-1} . The C–O–C ester linkage (1188 cm^{-1}) and C–H out of plane bending vibration (725 cm^{-1}) confirmed the ROP of CL by RB. The aromatic peaks corresponding to RB do not appear because of the low concentration of RB ([M/I] ratio = 100). Figure 1b represents the FTIR spectrum of RB-bridged diblock copolymer. Apart from the above-mentioned peaks, some new peaks are also observed. They are characterized below. The aromatic C–H symmetric and anti-symmetric stretching appeared at 2530 and 2655 cm^{-1} respectively. The peaks at 1686 and 1288 cm^{-1} confirmed the C=O stretching and aromatic ester C–O–C linkage of PAH respectively. PAH acts as a co-monomer to induce the ROP of THF in an aqueous medium. The aromatic C–H bending vibrations were noted at 666 and 793 cm^{-1} respectively. The peaks at 1403 and 1369 cm^{-1} correspond to the formation of the tetrahydrofuronium ion of PTHF. Thus, the appearance of new peaks confirms the ROP of THF in the presence of PAH using RB–PCL as a macro initiator. Recently, Murugesan et al. [22] observed similar results during the ROP of THF in the presence of PAH using poly(anthranilic acid) (PAA) as a macro initiator. Our results agree with them.

NMR studies

To confirm the structure of RB-initiated ROP of CL and THF, NMR spectra were recorded. Figure 2 represents the ^1H and ^{13}C -NMR spectra of the RB–PCL system. A peak at 4.22 ppm is formed due to the $-\text{OCH}_2$ protons (Fig. 2a). A peak at 2.4 ppm confirmed the $-\text{CO}_2\text{CH}_2$ protons. The peaks between 1 and 2 ppm confirmed the remaining protons of PCL. This is in accordance with the literature report [23, 24]. The peak at 0 ppm is due to the standard tetramethylsilane (TMS).

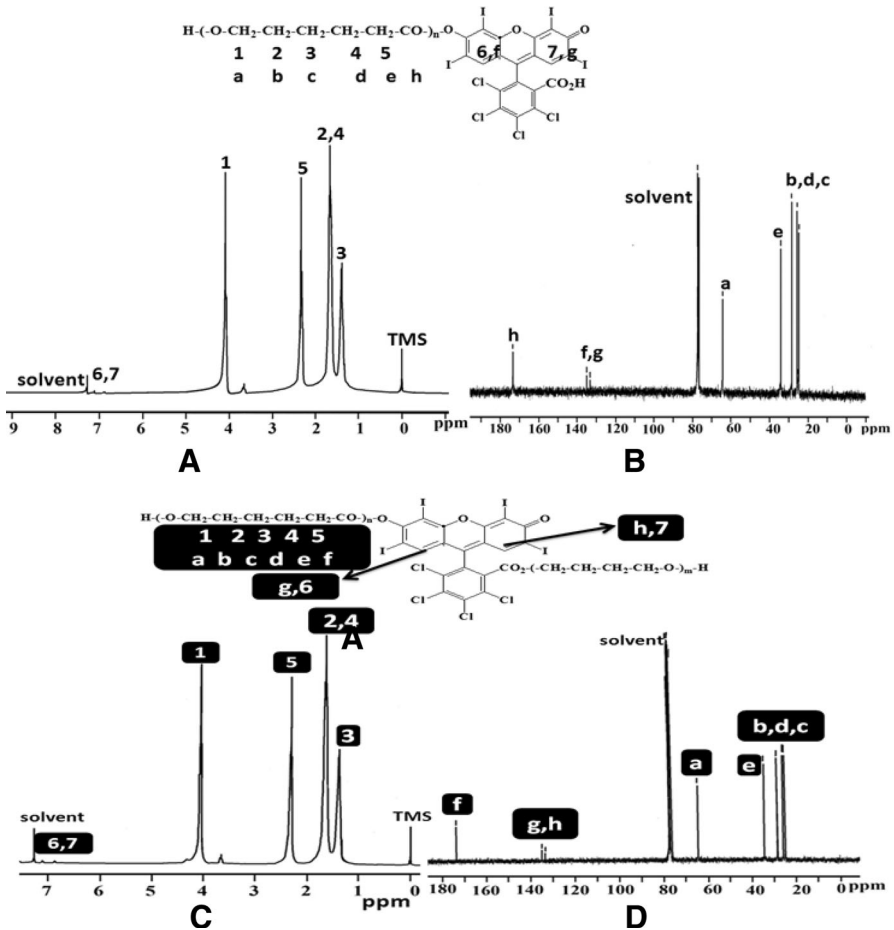


Fig. 2 ¹H-NMR spectrum of the PCL–RB system (a), ¹³C-NMR spectrum of the PCL–RB system (b), ¹H-NMR spectrum of the PCL–RB–PTHF system (c) and ¹³C-NMR spectrum of the PCL–RB–PTHF system (d)

The peak at 7.3 ppm is due to the deuterated chloroform used as solvent. Small humps at 6.9 and 7.1 ppm correspond to the aromatic protons of RB. This confirmed the ROP of CL by RB. Figure 2b represents the ¹³C-NMR spectra of the PCL–RB system. The peak at 173 ppm corresponds to the C=O signal. A small hump at 131 ppm is formed due to the aromatic carbon signals of RB. The –OCH₂ carbon signals of PCL appeared at 63 ppm. The –CO₂CH₂ carbon signal appeared at 34 ppm. The remaining carbon signals between 30 and 40 ppm match with the structure. Figure 2c, d indicates the ¹H-NMR and ¹³C-NMR spectra of the PCL–RB–PTHF system respectively. Here also peaks corresponding to PCL–RB appeared. No new peaks which corresponded to the PTHF and PAH segments were observed. This is due to the non-solvation effect of CDCl₃ for PTHF and PAH. The presence of PCL segments in the diblock copolymer shows the solubility in the

CDCl_3 solvent, but actually the PTHF or PAH segments are not solvated by the CDCl_3 solvent. Hence, the signals due to the PTHF and PAH segments are not shown.

UV–visible spectroscopy study

The UV–visible spectrum of pristine RB is given in Fig. 3a and shows two peaks. The peak at 545 nm corresponds to the monomeric form of RB, whereas a small shoulder at 507 nm is due to the dimeric structure of RB. In 2011, Chen et al. [25] reported that the Eosin Y, structurally similar to RB, initiated the ROP of CL. Eosin Y also has both a monomeric and dimeric structure. Figure 3b indicates the UV–visible spectrum of the PCL–RB system. Here, the system exhibits one absorption peak at 477.5 nm corresponding to the monomeric form of RB. The dimeric structure of RB disappeared due to the ROP of CL. This revealed that the dimerization or aggregation of RB dye was absent in the RB–PCL system [26]. After the ROP of CL, the absorption peak of RB was blueshifted due to the decrease in conjugation length of RB. The blueshift in the UV–visible spectrum confirmed the active participation of RB in the ROP of CL. The RB contains two functional groups, $-\text{OH}$ and $-\text{COOH}$. The $-\text{OH}$ group is more active toward the ROP of CL than $-\text{COOH}$. As a result, the $-\text{OH}$ group of RB is attached to the PCL chain. This is similar to that of Eosin Y–PCL system [25]. The broadening of the absorbance peak indicates the agglomeration of RB in the medium. Figure 3c denotes the UV–visible spectrum of the PCL–RB–PTHF system. Here also, the dimeric structure of RB has disappeared. The system exhibits an absorption peak at 477 nm corresponding to the monomeric structure of RB. The further blueshift in the absorption spectrum confirms the ROP of THF in the presence of PAH. The slight blueshift in the absorption spectrum can be explained as follows. The ROP of THF was carried out using RB–PCL as a macro initiator. The RB still contains one active carboxyl group.

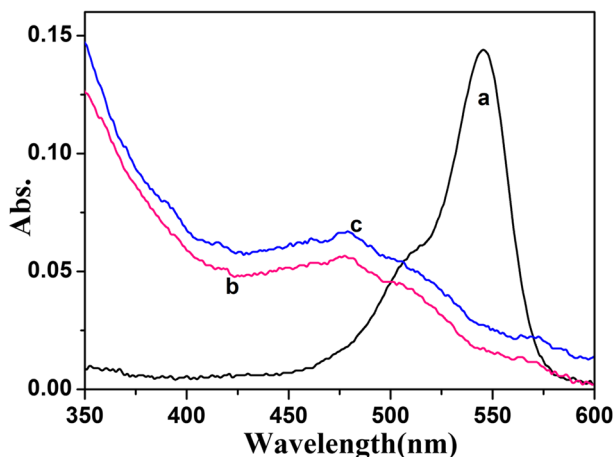


Fig. 3 UV–visible spectra of pristine RB (a), RB–PCL system (b) and PCL–RB–PTHF system (c)

The carboxyl group is more active toward the ROP of ether rather than the $-OH$ group of PCL. The stress via the incorporation of polymer chains on either side through the $-OH$ and the $-COOH$ groups destabilizes the optical property of RB. The blueshift in the absorption spectrum of RB also indicates the reduction in the size of the grafted polymer. This size reduction can further be supported by FESEM results. Here also, broadening of the peak was noticed due to the agglomeration of RB dye units. The dimeric structure of RB disappeared due to the ROP of CL, followed by THF in the presence of PAH.

Fluorescence emission study

The fluorescence emission spectrum of the RB–PCL system is given in Fig. 4a with a fluorescence emission intensity (FEI) value of 45 cps. The emission peak was noted at 522.2 nm. The fluorescence emission spectrum of the PCL–RB–PTHF system is shown in Fig. 4b. The system exhibits one emission peak at 527.9 nm with an FEI value of 32 cps. The results indicated that after the conjugation of the PCL–RB system with PTHF chains, the emission wavelength was redshifted slightly due to the formation of a new chemical linkage between the RB and PTHF chains. This is similar to the work of Chen et al. [25]. It means that the $-CO_2H$ group of RB is involved in the ROP of THF. In the preparation of the RB–PCL system, $[M/I] = 100$, whereas in the PTHF–RB–PCL system preparation, RB–PCL was used as an initiator in the same ratio. This includes the amount of both PCL and RB and hence the net quantity of RB was found to be reduced. Due to the difference in the molecular weight of the PCL–RB and PCL–RB–PTHF systems, automatically the emission intensity of the diblock copolymer is found to be low. The concentration of each system is mentioned in the experimental part. The molecular weights of the polymer systems are confirmed in the forthcoming GPC analysis section.

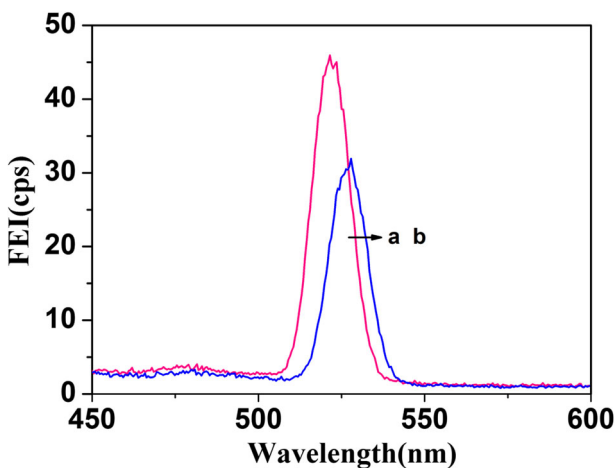


Fig. 4 Fluorescence emission spectra of the RB–PCL system (a) and PCL–RB–PTHF system (b)

DSC study

The primary aim of the DSC study is to analyze the influence of hydrophobic and hydrophilic segments on the phase transition temperature of the polymer. The thermal melt transition temperature of PCL was determined by DSC. Figure 5a represents the DSC scan of the RB–PCL system. The thermogram exhibits an endothermic peak at 67.1 °C corresponding to the melting of PCL chains. From the literature, it was found that the T_m of PCL varied slightly when varying the PCL chain end group and molecular weight of PCL [27, 28]. The DSC of PCL–RB–PTHF is given in Fig. 5b. The system exhibits one endothermic peak at 66.2 °C. The decrease in T_m is due to the introduction of THF segments into the RB–PCL chains. The T_m of PTHF varies between 48 and 65 °C [29]. There is no surprise in the T_m of the diblock copolymer, because both PCL and PTHF have low T_m values. Moreover, their T_m values overlap. It is well known that PCL is a semi-crystalline polymer. Here, the main aim is to analyze the T_m value of the diblock copolymer and not the crystallinity of the same.

TGA profile

The thermal stability of the homopolymer and diblock copolymer was studied with TGA. The TGA thermogram of the RB–PCL system is shown in Fig. 6a with three degradation steps. The first minor weight loss around 310 °C is due to break of the linkage between the RB and PCL chain. The second major weight loss around 385 °C is ascribed to the degradation of the PCL backbone. Recently, Kannammal et al. [30] found this type of degradation step for PCL. Our results coincide with their report. The minor weight loss around 500 °C is accounted by the degradation of RB with the evolution of carbon dioxide. It means, at lower temperature the

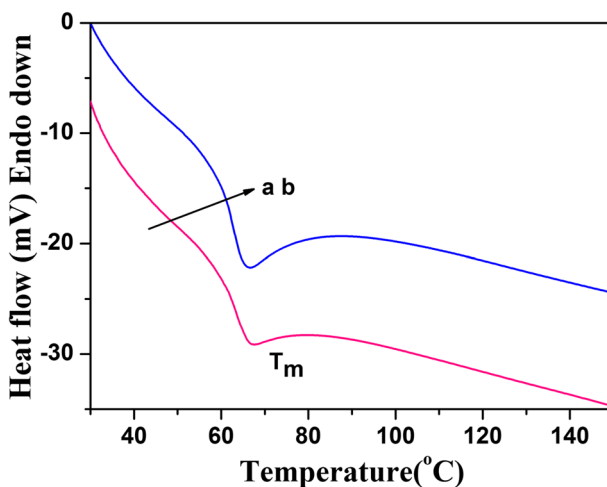


Fig. 5 DSC heating scan of the RB–PCL system (a) and PCL–RB–PTHF system (b)

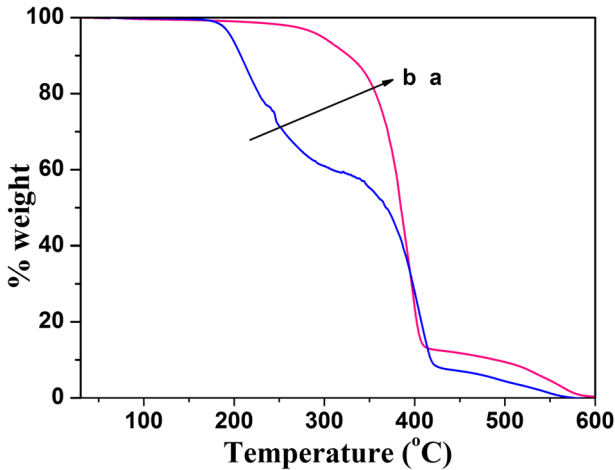


Fig. 6 TGA thermogram of the RB-PCL system (a) and PCL-RB-PTHF system (b)

linkage between the RB and PCL chain is broken, whereas at higher temperature (around 500 °C) the RB alone degrades. The TGA thermogram of the PCL-RB-PTHF system is given in Fig. 6b with a three-step degradation process. The first major weight loss around 242 °C is due to the degradation of PTHF segments present in the diblock copolymer. Our recent publication also confirmed the low degradation temperature (T_d) of the PTHF chains [29]. It also showed that the T_d of PTHF depends on the nature of the initiator used for ROP of THF. The second major weight loss around 391 °C is explained by the degradation of the PCL backbone [28, 30]. The third minor weight loss around 500 °C is again due to the degradation of the RB dye with the evolution of carbon dioxide. In comparison, the RB-PCL system exhibited higher thermal stability than the PCL-RB-PTHF system due to the hydrophobic nature. Hence, the appearance of a separate degradation process confirmed the ROP of THF in the presence of PAH using RB-PCL as a macro initiator. Even then, the PTHF chains are hydrophilic in nature, and there is no separate weight loss peak corresponding to the moisture. Above all, PTHF itself has very low degradation temperature [29].

SEM analysis

The surface morphology of RB-initiated ROP of CL is shown in Fig. 7a. The image exhibits the presence of some microvoids on the surface of PCL. The length of the voids varied from 0.1 to 1 μm . The appearance of microvoids confirmed the possible biomedical application of PCL as a drug carrier [22]. Generally, a drug carrier requires a polymer with sufficient molecular weight with some functional groups to hold the drug molecules via hydrogen bonding, presence of microvoids to temporarily accommodate the drug moieties and the existence of biocompatibility. The present polymer system satisfies the last two requirements and is hence suitable for drug carrier application. Figure 7b indicates the SEM image of the RB-

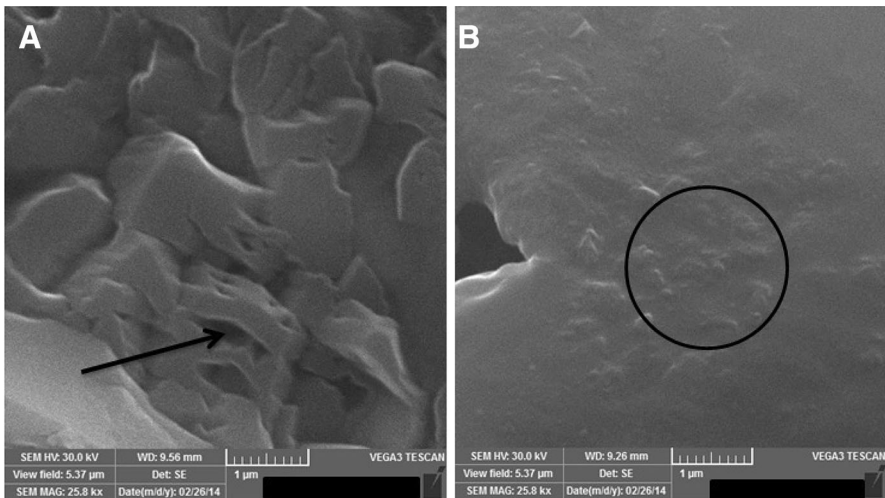


Fig. 7 SEM images of the RB–PCL system (a, b)

PCL system. Here, one can see the presence of some polymer nanoparticles of size approximately 100 nm. The appearance of polymer nanoparticle is the novelty of the present investigation. The polymer nanoparticles are responsible for an effective drug carrying or releasing application.

FESEM analysis

The FESEM image of the PCL–RB–PTHF system is given in Fig. 8. Figure 8a represents the broken stone-like morphology with microvoids corresponding to the PCL morphology [23, 28]. Figure 8b shows the FESEM image of the PCL–RB–PTHF system with more polymer nanoparticle formation with size less than 50 nm. The polymer nanoparticle formation can be explained as follows: the hydrophobic

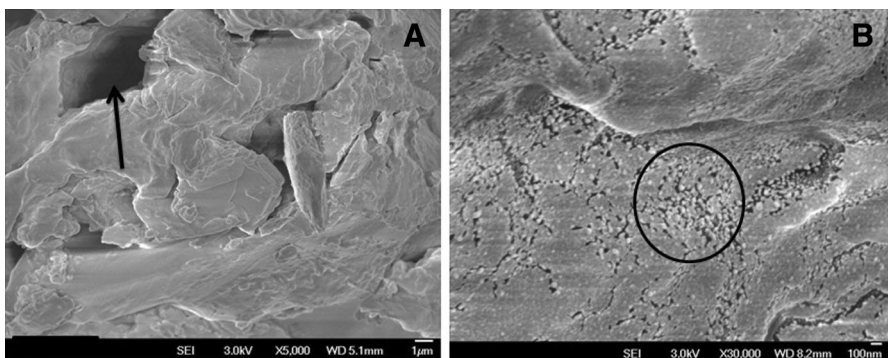


Fig. 8 FESEM image of the RB–PCL system (a) and PCL–RB–PTHF system (b)

PCL and the hydrophilic PTHF are attached through RB. Hence, there will be formation of nano particles in the interface region between the hydrophobic and hydrophilic regions. The conjugation of hydrophobic and hydrophilic segments leads to the self-assembly process. That is, hydrophilic PTHF segments act as a core, whereas the hydrophobic PCL segments act as a shell-like structure. Self-assembly of the amphiphilic structure led to the formation of polymer nanoparticles. Again, this proved the biomedical application of the amphiphilic copolymer, particularly as a drug carrier.

GPC analysis

The ROP of CL and THF in the presence of RB was confirmed by GPC analysis. Figure 9a indicates the GPC trace of the RB–PCL system. From the image, the M_w , M_n and polydispersity (PD) values were calculated as 2594.8 g/mol, 1365.2 and 1.9 respectively. This confirmed the presence of 22 repeating units in the PCL chain. Here, $[M/I] = 100$. In the literature, it has been reported that the structurally similar xanthene-type dye (i.e.,) Eosin Y produced M_w of 3856 g/mole for PCL [27]. This proves that the ROP initiating efficiency of a dye molecule depends on the structure, substituents present on the dye molecule and the nature of the functional group involved in the ROP process. The PD value indicated the absence of crosslinking and branching during the ROP process of CL. This proved that RB was a good initiator for the ROP of CL. Figure 9b indicates the GPC trace of the PCL–RB–PTHF system with the M_w , M_n and PD values as 3211 g/mol, 1783.8, and 1.8 respectively. Again, the PD value confirmed the absence of crosslinking and branching. The increase in M_w confirmed the ROP of THF in the presence of RB–PCL as a macro initiator. The difference in the M_w values indicated that ten repeating units of THF are present in the diblock copolymer. The increase in molecular weight co-supported both DSC and TGA results. The homo PCL contains 22 repeating units of CL, whereas in the copolymer also the same number of CL repeating units must be present. In addition, some THF with PAH repeating units is present. Thus, the increase in molecular weight of the copolymer confirmed the

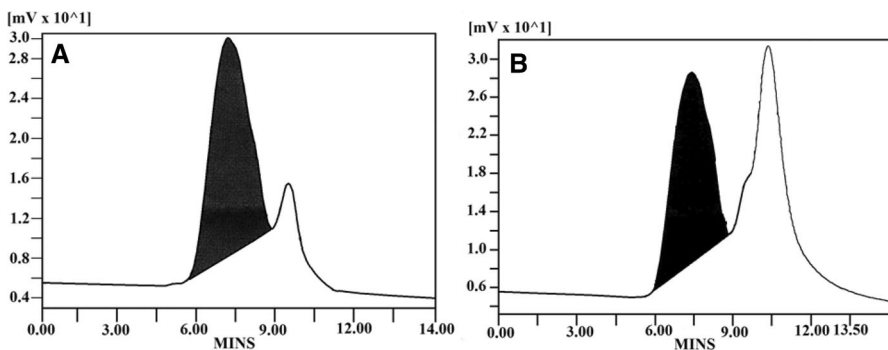


Fig. 9 GPC trace of the RB–PCL system (a) and PCL–RB–PTHF system (b)

ROP of THF in the presence of PAH by using RB–PCL as a macro initiator. The molecular weight determination by $^1\text{H-NMR}$ is not useful, because the diblock copolymer is not solvated in CDCl_3 solvent. Hence, peaks corresponding to the THF segments are absent. But both the homopolymer and the diblock copolymer are soluble in the THF solvent. Hence, GPC measurement is possible. For the dissolution of diblock copolymer, one cannot use trifluoroacetic acid because it degrades the structure of the copolymer. The degradation of the structure will lead to the decrease in molecular weight of the diblock copolymer. This can be explained on the basis of strong acidic pH.

EDX report

Figure 10 represents the EDX spectrum of the RB–PCL system. The presence of Cl and I peaks confirmed the attachment of RB to PCL chains. The appearance of carbon and oxygen peaks indicated the ROP of CL by RB. The percentage contents of C, O, I and Cl are 75.06, 19.87, 2.53 and 2.54 % respectively. The Cl and I content confirmed the attachment of RB to one end of PCL.

Band gap study

From the UV–visible absorbance (Fig. 3) spectrum, one can easily find out the band gap using Tauc's plot. Figure 11a indicates the Tauc's plot of pristine RB with a band gap value of 4.36 eV. Figure 11b, c represents the Tauc's plot of RB–PCL and PCL–RB–PTHF systems respectively, with band gap values of 4.49 and 4.54 eV. It is very interesting to note that while increasing the molecular weight of the polymer, the band gap value is increased correspondingly; i.e., when the M_w of PCL attached to RB was 2594.8 g/mol, the band gap value was determined as 4.49 eV. After the

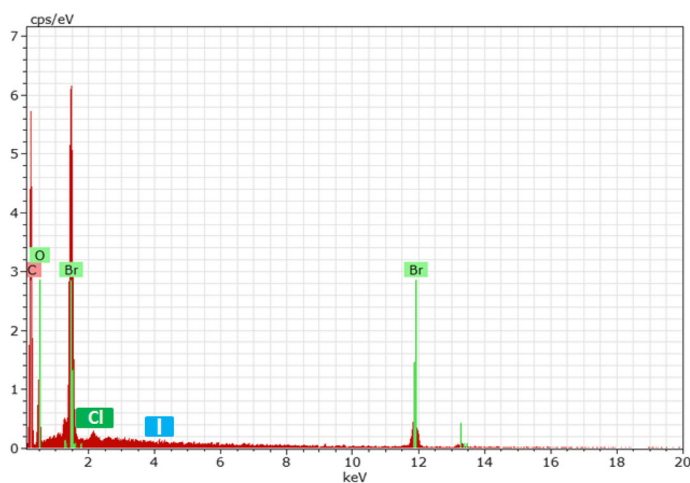


Fig. 10 EDX spectrum of the RB–PCL system

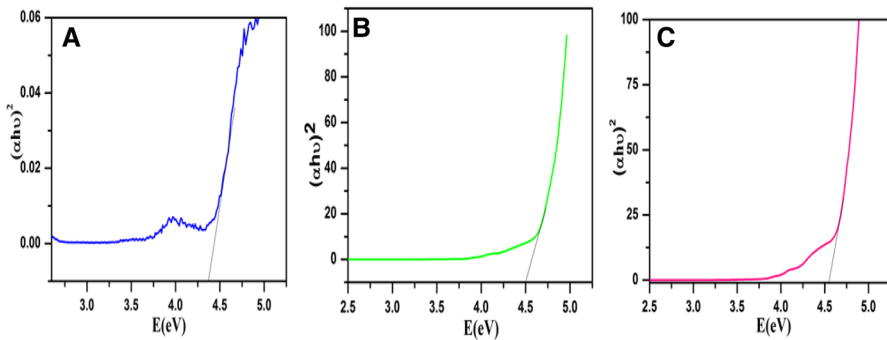


Fig. 11 Tauc's plot for the pristine RB (a), PCL–RB (b) and PCL–RB–PTHF (c) systems

diblock copolymerization, the M_w increased to 3211 g/mol with the band gap value of 4.54 eV. The influence of M_w of the polymer on the band gap value is under further investigation in our laboratory. Generally, it can be explained as follows: While increasing the molecular weight of the polymer, there will be an increase in coil structure. This coil structure leads to the encapsulation of the bridging agent. As a result of an encapsulation, more stress is enforced on the RB in the opposite direction due to diblock copolymerization.

In the present investigation, a fluorescent biodegradable synthetic polymer was prepared by the bulk polymerization method. It is well known that both PCL and PTHF have lower T_m . Polymers with lower processing temperature have wide application as a bioprobe in the biomedical engineering field. We tried to synthesize such a biomedical candidate. PTHF has lower T_d than PCL. The interface region between the hydrophobic PCL and hydrophilic PTHF led to the formation of polymer nanoparticles. The nanoparticle is a key element for an efficient drug delivery process. The FESEM results confirmed polymer nanoparticle formation.

Conclusions

In the present work, a diblock copolymer from CL and THF was prepared with RB as the bridging agent. Both the FTIR and UV–visible studies confirmed the ROP of CL and THF in the presence of RB and in the presence of PAH. The TGA study of the polymer systems clearly indicated the higher thermal stability of RB–PCL system than the PCL–RB–PTHF system due to the hydrophobic nature of the former. The DSC thermograms of RB–PCL and PCL–RB–PTHF systems exhibited endothermic peaks at 67.1 and 66.2 °C respectively, corresponding to the melting of PCL and PTHF chains, and the decrease in T_m of the latter is due to the introduction of THF segments into the RB–PCL chains. The surface morphology of RB-initiated ROP of CL exhibited some micro voids on the surface of PCL and some polymer nanoparticles of size approximately 100 nm which confirmed the suitability of PCL as a drug carrier in biomedical application. The FESEM image of the PCL–RB–PTHF system showed more polymer nanoparticle formation with size less than

50 nm, which further confirmed the application of the copolymer as a drug carrier. The PD value from the GPC study indicated the absence of branching and crosslinking in both systems, and the increase in M_w of the PCL–RB–PTHF system was attributed to the introduction of THF into the RB–PCL system. Proton and carbon NMR spectra clearly confirmed that RB initiated ROP of CL.

Acknowledgments We express our sincere thanks to Dr. N. Sundararajan, Associate Professor of English department, KCET for his valuable help with the manuscript.

References

1. Wang J, Yao K, Wang C, Tang C, Jiang X (2013) Synthesis and drug delivery of novel amphiphilic block copolymers containing hydrophobic dehydroabietic moiety. *J Mater Chem B* 1:2324–2332
2. Wang F, Bronich TK, Kabanov AV, Rauh RD, Roovers J (2005) Synthesis and evaluation of a star amphiphilic block copolymer from poly(ϵ -caprolactone) and poly(ethylene glycol) as a potential drug delivery carrier. *Bioconjug Chem* 16:397–405
3. Li XH, Zhang DH, Chen JS (2006) Synthesis of amphiphilic superparamagnetic ferrite/block copolymer hollow microspheres. *J Am Chem Soc* 128:8382–8383
4. Chae CG, Shah PN, Min J, Seo HB, Lee JS (2014) Synthesis of novel amphiphilic polyisocyanate block copolymer with hydroxyl side group. *Macromolecules* 47:1563–1569
5. Nemiche N, Sebba FZ, Kada SO (2014) Synthesis, characterization and self-assembly of amphiphilic block copolymer poly(4-vinyl benzene chloride)-*b*-poly(*N*-vinylpyrrolidone) in aqueous solution. *Res Chem Intermed* 40:3127–3134
6. Shah M, Ullah N, Choi MH, Kim MO, Yoon SC (2012) Amorphous amphiphilic P(3HV-*co*-4HB)-*b*-mPEG block copolymer synthesized from bacterial copolyester via melt transesterification: nanoparticle preparation, cisplatin-loading for cancer therapy and in vitro evaluation. *Eur J Pharm Biopharm* 80:518–527
7. Lu Y, Hu Y, Wang ZM, Manias E, Chung TC (2002) Synthesis of new amphiphilic diblock copolymers containing poly(ethylene oxide) and poly(α -olefin). *J Polym Sci Part A Polym Chem* 40:3416–3425
8. Bajpai A, Dixit N (2005) Synthesis of amphiphilic block copolymer of butadiene and acrylamide using telechelic polybutadiene and V (V) as redox system. *J Macromol Sci Part A Pure Appl Chem* 42:993–1012
9. Zhu YJ, Tan YB, Du X (2008) Preparation and self-assembly behavior of polystyrene-block-poly(dimethylaminoethyl methacrylate) amphiphilic block copolymer using atom transfer radical polymerization. *Express Polym Lett* 2:214–225
10. Cui C, Bonder EM, Qin Y, Jäkle F (2010) Synthesis and solvent-dependent micellization of the amphiphilic block copolymer poly(styreneboronicacid)-block-polystyrene. *J Polym Sci Part A Polym Chem* 48:2438–2445
11. Murugesan A, Meenarathi B, Kannammal L, Palanikumar S, Anbarasan R (2014) Synthesis, characterization and drug delivery activity of poly(anthranilicacid) based triblock copolymer. *Synth Met* 189:143–151
12. Gardella L, Cavallo D, Colonna S, Fina A, Monticelli O (2014) Novel poly(l-lactide)/poly(d-lactide)/poly(tetrahydrofuran) multiblock copolymers with a controlled architecture: synthesis and characterization. *J Polym Sci Part A Polym Chem* 52:3269–3282
13. Kušan J, Keul H, Höcker H (2001) Block copolymers comprising a polytetrahydrofuran block and one or two [5]-polyurethane block(s): synthesis and characterization. *e-Polym* 11:1–9
14. Alemseghed MG, Gowrisanker S, Servello J, Stefan MC (2009) Synthesis of di-block copolymers containing regular poly(3-hexylthiophene) and poly(tetrahydrofuran) by a combination of Grignard metathesis and cationic polymerizations. *Macromol Chem Phys* 210:2007–2014
15. Fan WW, Fan XD, Tian W, Liao XQ, Zhang WB, Mu CG, Kong J (2013) Poly(ethylene glycol)-poly(tetrahydrofuran)-poly(ethylene glycol) triblock copolymer: synthesis, crystallization behavior and novel morphology. *Express Polym Lett* 7:416–430
16. Panzarini E, Inguscio V, Dini L (2011) Overview of cell death mechanisms induced by rose bengal acetate-photodynamic therapy. *Int J Photoener* 2011:1–11

17. Chodosh J, Banks MC, Stroop WG (1992) Rose Bengal inhibits Herpes simplex virus replication in vero and human corneal epithelial cells in vitro. *Invest Ophthalmol Vis Sci* 33:2520–2527
18. Pretorius PJ, Jansen CR, Simson IW, Wittmann W (1968) Application of the radio-iodine rose bengal test in liver disease in infancy and childhood. *S A Med J* 1:147–153
19. Sandholzer M, Lex A, Trimmel G, Saf R, Stelzer F, Slugovc C (2007) Xanthene dye functionalized norbornenes for the use in ring opening metathesis polymerization. *J Polym Sci Part A Polym Chem* 45:1336–1348
20. Schap AP, Thayer AL, Blossey EC, Neckers DC (1975) Polymer-based sensitizers for photo-oxidations. II. *J Am Chem Soc* 97:3741–3745
21. Meenarathi B, Palanikumar S, Kannammal L, Anbarasan R (2014) Synthesis, characterization and catalytic activity of Ag-acidfuchsin nanohybrid system towards the ring opening polymerization of ϵ -caprolactone. *Spectrochim Acta A Mol Biomol Spectrosc* 135:93–100
22. Murugesan A, Meenarathi B, Kannammal L, Palanikumar S, Anbarasan R (2014) Synthesis, characterization and drug delivery activity of poly(sulphanilic acid) based triblock copolymer. *Russ J Appl Chem (under review)*
23. Meenarathi B, Chen HH, Chen PH, Anbarasan R (2014) Synthesis and characterization of fluorescent biodegradable poly(ϵ -caprolactone). *Int J Plast Technol* 18:135–145
24. Meenarathi B, Chen HH, Chen PH, Anbarasan R (2013) Near infrared dye functionalized MWCNT as an effective initiator for the ring opening polymerization of ϵ -caprolactone. *J Polym Res* 20:118–130
25. Chen HH, Anbarasan R, Chen PH (2011) Synthesis and characterizations of novel acid functionalized and fluorescent poly(ϵ -caprolactone). *J Mater Sci* 46:1796–1805
26. Shrestha A, Hamblin MR, Kishen A (2012) Characterization of conjugate between rose bengal and chitosan for targeted antibiofilm and tissue stabilization effects as a potential treatment of infected dentin. *Antimicrob Agents Chemother* 56:4876–4884
27. Chen HH, Anbarasan R, Kuo LS, Chen PH (2011) A novel report on Eosin Y functionalized MWCNT as an initiator for the ring opening polymerization of ϵ -CL. *Mater Chem Phys* 126:584–590
28. Meenarathi B, Kannammal L, Palanikumar S, Anbarasan R (2014) Synthesis and characterizations of Fe₃O₄-acid fuchsin tagged poly(ϵ -caprolactone) nanocomposites. *Mater Res Exp* 1:1–16
29. Ramkumar P, Ragunathan M, Parthiban R, Maranathan R, Anbarasan R (2014) Synthesis and characterization of mercaptoacid initiated ring opening polymerization of tetrahydrofuran. *Int J Chem Biol Sci* 1:1–9
30. Kannammal L, Palanikumar S, Meenarathi B, Yelilarasi A, Anbarasan R (2014) Synthesis, characterization and band gap energy of poly(ϵ -caprolactone)/Sr-MSA nano-composite. *J Phys D Appl Phys* 47:1–10